

OBSERVABILITY OF THE GENERAL RELATIVISTIC PRECESSION OF PERIASTRA IN EXOPLANETS

ANDRÉS JORDÁN^{1,2,3} AND GÁSPÁR Á. BAKOS^{1,4}

Accepted for publication in ApJ

ABSTRACT

The general relativistic precession rate of periastra in close-in exoplanets can be orders of magnitude larger than the magnitude of the same effect for Mercury. The realization that some of the close-in exoplanets have significant eccentricities raises the possibility that this precession might be detectable. We explore in this work the observability of the periastra precession using radial velocity and transit light curve observations. Our analysis is independent of the source of precession, which can also have significant contributions due to additional planets and tidal deformations. We find that precession of the periastra of the magnitude expected from general relativity can be detectable in timescales of $\lesssim 10$ years with current observational capabilities by measuring the change in the primary transit duration or in the time difference between primary and secondary transits. Radial velocity curves alone would be able to detect this precession for super-massive, close-in exoplanets orbiting inactive stars if they have ~ 100 datapoints at each of two epochs separated by ~ 20 years. We show that the contribution to the precession by tidal deformations may dominate the total precession in cases where the relativistic precession is detectable. Studies of transit durations with *Kepler* might need to take into account effects arising from the general relativistic and tidal induced precession of periastra for systems containing close-in, eccentric exoplanets. Such studies may be able to detect additional planets with masses comparable to that of Earth by detecting secular variations in the transit duration induced by the changing longitude of periastron.

Subject headings: celestial mechanics — planetary systems

1. INTRODUCTION

Following the discovery of an extra-solar planet around the solar type star 51 Pegasi (Mayor & Queloz 1995) there has been rapid progress in the detection and characterization of extra-solar planetary systems. The very early discoveries have shattered our view on planetary systems, as certain systems exhibited short periods (51 Peg), high eccentricities (e.g. 70 Virginis b, Marcy & Butler 1996), and massive planetary companions (e.g. Tau Boo b, Butler et al. 1997).

Interestingly, systems with all these properties combined (i.e. massive planets with short periods, small semi-major axes, high eccentricities) have been also discovered (e.g., HAT-P-2b, XO-3b; Bakos et al. 2007; Johns-Krull et al. 2008). The high eccentricities are somewhat surprising, as hot Jupiters with short periods are generally expected to be circularized in timescales shorter than the lifetime of the system if the parameter Q , inversely proportional to the planet's tidal dissipation rate, is assumed to be similar to that inferred for Jupiter (Goldreich & Soter 1966; Rasio et al. 1996).

By virtue of their small semi-major axes and high eccentricities, the longitude of periastron ω of some of the newly discovered systems are expected to precess due to General Relativistic (GR) effects at rates of degrees per century. This is orders of magnitude larger than the same effect observed in Mercury in our Solar System ($43''/\text{century}$), which offered one of the cornerstone tests of GR. Furthermore, the massive, close-in eccentric planets induce significant reflex motion of the host star, therefore enhancing the detectability of the precession directly via radial velocities.

In this work we explore the observability of the precession of the longitude of periastron with the magnitude expected from GR in exoplanets using radial velocity and transit timing observations. We also consider in this work the periastra precession due to planetary perturbers and tidal deformations, which can have contributions comparable or greater than that of GR. Previous works (Miralda-Escudé 2002; Heyl & Gladman 2007) have explored some aspects of the work presented here in the context of using timing observations to detect terrestrial mass planets. We refer the reader to independent work by Pál & Kocsis (2008) that also explores the measurable effects of the periastra precession induced by GR.

2. EXPECTED PRECESSION OF PERIASTRA

Before continuing let us fix our notation. In what follows a will denote the semi-major axis of the Keplerian orbit of the planet-star separation, e its eccentricity, P its period, ω its longitude of periastron, M_\star and R_\star the mass and radius of the host star, respectively, and $n \equiv (GM_{\text{tot}}/a^3)^{1/2}$ is the Keplerian mean motion (orbital angular frequency),

¹ Harvard-Smithsonian Center for Astrophysics, 60 Garden St., Cambridge, MA 02138; ajordan@cfa.harvard.edu, gbakos@cfa.harvard.edu.

² Clay Fellow.

³ Departamento de Astronomía y Astrofísica, Pontificia Universidad Católica de Chile, Casilla 306, Santiago 22, Chile.

⁴ NSF Postdoctoral Fellow.

TABLE 1
GR PRECESSION OF EXOPLANETS WITH $e > 0.1$ AND GR PRECESSION RATES
> $1^\circ/\text{CENTURY}$

Name	a (AU)	e	M_\star (M_\odot)	Period (days)	K (m sec $^{-1}$)	ω (deg)	$\dot{\omega}_{\text{GR}}$ °/century	TEP?
HD49674 b	0.058	0.290	1.060	4.944	13.7	283.0	1.576	0
HD88133 b	0.047	0.133	1.200	3.416	36.1	349.0	2.958	0
GJ 436 b	0.028	0.159	0.410	2.644	18.7	339.0	2.234	1
HD118203 b	0.070	0.309	1.230	6.133	217.0	155.7	1.231	0
HAT-P-2 b	0.069	0.507	1.350	5.633	884.0	184.6	1.836	1
HD185269 b	0.077	0.296	1.280	6.838	90.7	172.0	1.046	0
XO-3 b	0.048	0.260	1.410	3.192	1471.0	-15.4	3.886	1

where G is Newton's gravitational constant and $M_{\text{tot}} = M_\star + M_p$ with M_p the mass of the planet. The reflex motion of the host star is characterized in a similar manner. In this section we detail the expected mechanisms that will cause a precession in the value of ω .

2.1. General Relativistic Precession

One of the most well-known consequences of General Relativity is that orbits in a Schwarzschild metric are no longer closed as is the case for the Kepler problem in Newtonian mechanics. The rate of precession of the longitude of periastron due to GR is given to leading post-Newtonian order by

$$\dot{\omega}_{\text{GR}} = \frac{3GM_\star}{ac^2(1-e^2)}n \quad (1)$$

(see any general relativity textbook, e.g. Misner et al. 1973, for a derivation). With a expressed in astronomical units, P in days and the mass of the host star M_\star in solar units, $\dot{\omega}_{\text{GR}}$ is given in units of degrees per century by

$$\dot{\omega}_{\text{GR}} = \frac{7.78}{(1-e^2)} \left(\frac{M_\star}{M_\odot} \right) \left(\frac{a}{0.05\text{AU}} \right)^{-1} \left(\frac{P}{\text{day}} \right)^{-1} \quad [^\circ/\text{century}]. \quad (2)$$

We use equation 2 to estimate the expected precession for currently known exoplanets as listed in the online California & Carnegie Catalog of Exoplanets (Butler et al. 2006, version Nov 7 2007). We list in Table 1 all exoplanets that have $e > 0.1$ and that have $\dot{\omega}_{\text{GR}} > 1^\circ/\text{century}^5$. From left to right, the columns in Table 1 record the name of the exoplanet, its semi-major axis, its eccentricity, the mass M_\star of the host star, the period, the velocity amplitude⁶, the longitude of periastron ω , the calculated $\dot{\omega}_{\text{GR}}$ and finally a flag that is 1 if the planet is transiting its host star and 0 otherwise. The condition on e is in order to consider only systems where GR effects can be constrained with sufficient confidence. Additionally, we restrict ourselves to stars which have evidence currently for a single exoplanet in order to avoid the complications arising from the precession of ω induced by other planets (see below)⁷. We have added to the exoplanets listed by Butler et al. (2006) the recently discovered XO-3b (Johns-Krull et al. 2008), which has the largest predicted $\dot{\omega}_{\text{GR}}$ of all exoplanets listed in Table 1.

As can be seen in Table 1, seven systems have $\dot{\omega}_{\text{GR}} > 1^\circ/\text{century}$, with 3 of them being transiting systems. In timescales of a few tens of years, the longitude of periastron of the systems is expected to shift in these systems by $\delta\omega \gtrsim 0.5^\circ$, a change that, as we will show below, may produce detectable effects. GR effects are not the only mechanisms that can cause a shift in ω though, so we now turn our attention to additional mechanisms.

2.2. Stellar Quadrupole, Tides and Additional Planets

Besides the GR precession discussed above, ω can precess due to the presence of additional effects. Miralda-Escudé (2002) discussed the observability, using the duration of transits and the period between transits, of changes in ω caused by a stellar quadrupole moment and perturbations from other planets. These effects, some of which were discussed using more accurate calculations by Heyl & Gladman (2007), may additionally cause a precession of the orbital plane. Additionally, tidal deformations induced on the star and the planet can also produce a secular change on ω , an effect not considered in the studies mentioned above. The effect of apsidal motions induced by tidal deformations is a well known effect in eclipsing binaries (Sterne 1939; Quataert et al. 1996; Smeyers & Willems 2001), and was included in

⁵ The magnitude of all the effects discussed in what follows where $\dot{\omega}_{\text{GR}}$ would manifest itself are increasing functions of e . Systems with low e are therefore not relevant from the point of view of detecting GR effects. Heyl & Gladman (2007) presents in their Figure 4 an estimate of $\dot{\omega}_{\text{GR}}$ for all systems in Butler et al. (2006) and note the four systems with higher values. None of those are in Table 1 because they all have $e < 0.03$.

⁶ This is often referred to as the semi-amplitude in the exoplanet literature. We choose to use simply amplitude in this paper in order to agree with the widespread usage in the physical sciences for the multiplicative factor in a simple harmonic oscillator.

⁷ Adams & Laughlin (2006a,b) studied the effects of secular interactions in multiple-planet systems including the effects of GR. They show that GR can have significant effects on secular perturbations for systems with favorable characteristics.

the analysis of the planetary system around HD 83443 by Wu & Goldreich (2002). Tidal deformations can produce a significant amount of precession in close-in exoplanets and should therefore be taken into account.

The precession caused by a stellar quadrupole moment is given to second order in e and first order in $(R_*/a)^2$ by

$$\dot{\omega}_{\text{quad}} \approx \frac{3J_2 R_*^2}{2a^2} n, \quad (3)$$

where J_2 is the quadrupole moment (Murray & Dermott 1999). In units of degree/century this expression reads

$$\dot{\omega}_{\text{quad}} \approx 0.17 \left(\frac{P}{\text{day}} \right)^{-1} \left(\frac{J_2}{10^{-6}} \right) \left(\frac{R_*}{R_\odot} \right)^2 \left(\frac{a}{0.05 \text{AU}} \right)^{-2} \quad [^\circ/\text{century}]. \quad (4)$$

It is clear from this equation that for values of $J_2 \lesssim 10^{-6}$ similar to that of the Sun (Pireaux & Rozelot 2003) the value of $\dot{\omega}_{\text{quad}}$ is smaller than the value of $\dot{\omega}$ expected from GR (see also Miralda-Escudé 2002). We will therefore assume in what follows that $\dot{\omega}_{\text{quad}}$ is always negligible in comparison with $\dot{\omega}_{\text{GR}}$.

The tidal deformations induced on the star and the planet by each other will lead to a change in the longitude of periastron which is given, under the approximation that the objects can instantaneously adjust their equilibrium shapes to the tidal force and considering up to second order harmonic distortions, by

$$\dot{\omega}_{\text{tide}} \approx \frac{15f(e)}{a^5} \left(\frac{k_{2,s} M_p R_*^5}{M_*} + \frac{k_{2,p} M_* R_p^5}{M_p} \right) n, \quad (5)$$

where $f(e) \equiv (1 - e^2)^{-5} [1 + (3/2)e^2 + (1/8)e^4]$, and $k_{2,s}, k_{2,p}$ are the apsidal motion constants for the star and planet respectively, which depend on the mass concentration of the tidally deformed bodies (Sterne 1939). For stars we expect $k_{2,s} \lesssim 0.01$ (Claret & Gimenez 1992), while for giant planets we expect $k_{2,p} \approx 0.25$ if we assume that their structure can be roughly described by a polytrope of index $n \approx 1$ (Hubbard 1984). For the extreme case of a sphere of uniform mass density, the apsidal motion constant takes the value $k_2 = 0.75$ (e.g., Smeyers & Willems 2001). We see from Equation 5 that for close-in hot Jupiters the term containing $k_{2,p}$ will dominate, and that the effect of tides on ω increases very rapidly with decreasing a . In units of degree/century equation 5 gives

$$\dot{\omega}_{\text{tide}} \approx 1.6f(e) \mathcal{T} \left(\frac{P}{\text{day}} \right)^{-1} \left(\frac{k_{2,p}}{0.1} \right) \left(\frac{a}{0.05 \text{AU}} \right)^{-5} \left(\frac{R_p}{R_J} \right)^5 \left(\frac{M_J}{M_p} \right) \left(\frac{M_*}{M_\odot} \right) \quad [^\circ/\text{century}], \quad (6)$$

where we have introduced $\mathcal{T} \equiv 1 + (R_*/R_p)^5 (M_p/M_*)^2 (k_{2,s}/k_{2,p})$, which is ≈ 1 for the case of a close-in Jupiter. Assuming that $k_{2,p} \sim 0.1$, $e \lesssim 0.5$, $M_p \sim M_J$, $M_* \sim M_\odot$, $R_* \sim R_\odot$ and $R_p \sim R_J$ it follows that $\dot{\omega}_{\text{tide}}$ is of comparable magnitude as $\dot{\omega}_{\text{GR}}$.

The precession of the periastra caused by a second planet, which we dub a “perturber”, is given to first order in e and lowest order in (a/a_2) by

$$\dot{\omega}_{\text{perturber}} \approx \frac{3M_2 a^3}{4M_* a_2^3} n \quad (7)$$

(Murray & Dermott 1999; Miralda-Escudé 2002), where M_2 is the mass of the second planet and a_2 the semi-major axis of its orbit. In terms of deg/century this expression reads

$$\dot{\omega}_{\text{perturber}} \approx 29.6 \left(\frac{P}{\text{day}} \right)^{-1} \left(\frac{a}{a_2} \right)^3 \left(\frac{M_*}{M_\odot} \right)^{-1} \left(\frac{M_2}{M_\oplus} \right) \quad [^\circ/\text{century}]. \quad (8)$$

For a perturber with $a_2 = 2a$ and a mass similar to Earth orbiting a solar-mass star, we get that $\dot{\omega}_{\text{perturber}} \sim 3 \times 10^{-7} n$ or $\dot{\omega}_{\text{perturber}} \sim 0.7$ deg/century for a $P = 5$ days planet. This is comparable to the precession expected from GR and therefore any detected precession of the longitude of periastron will be that of GR plus the possible addition of any perturber planet present in the system and the effects of tidal deformations (and generally a negligible contribution from the stellar quadrupole).

In what follows we will discuss the observability of changes in ω using radial velocity and transit observations. As just shown, any precession is expected to arise by GR, the effect of additional planets or tidal deformations. The discussion that follows addresses the detectability of changes in ω independent of their origin.

3. OBSERVABILITY OF PERIASTRA PRECESSION IN EXTRA-SOLAR PLANETS

3.1. Radial Velocities

The radial velocity of a star including the reflex motion due to a planetary component is given by

$$v_r(t) = v_0 + K[\cos(\omega + f(t - t_0)) + e \cos(\omega)], \quad (9)$$

where v_0 is the systemic velocity, t_0 the time coordinate zeropoint, f the true anomaly and K is the velocity amplitude which is related to the orbital elements and the masses by

$$K = \left(\frac{2\pi G}{P} \right)^{1/3} \frac{M_p \sin i}{M_{\text{tot}}}, \quad (10)$$

TABLE 2
RESULTS OF RADIAL VELOCITY CURVES FIT
SIMULATIONS FOR $N_{\text{obs}} = 100$, $\sigma_{\text{obs}} = 2$
M/SEC AND $\sigma_{\text{jitter}} = 4$ M/SEC

K (m sec ⁻¹)	e	σ_{ω} (deg)	α_{20} (deg/century)
100	0.10	3.77	80.010
100	0.20	1.85	39.204
100	0.30	1.29	27.457
100	0.40	1.05	22.249
100	0.50	0.95	20.253
100	0.60	0.86	18.159
1000	0.10	0.38	8.059
1000	0.20	0.19	4.106
1000	0.30	0.13	2.768
1000	0.40	0.10	2.182
1000	0.50	0.09	1.959
1000	0.60	0.08	1.790

where i is the orbit inclination. Fitting for the observed radial velocities of a star will give then direct estimates of v_0, t_0, K, e, P and ω .

Our aim in this section is to determine if ω can be constrained tightly enough in timescales of tens of years or less in order to detect changes in ω of the magnitude produced by GR in those time-spans. In order to do this we have simulated data and then fit it with a model of the form given by equation 9 a total of 1000 times. We then recover the best-fit values of ω in all simulations and use that to estimate the probability distribution $\phi(\omega)$ expected under given assumptions.

The systemic velocity v_0 and t_0 are just zero-points that we set to 0 in all our simulations, where we also set the time units such that $P = 1$ (note though that we do fit for all these quantities so that their effect on the fit propagates to the uncertainties of ω). By trying several values of ω we have verified that the probability distributions recovered do not depend strongly on the particular value of ω , which we therefore fix for all simulations at an arbitrary value $\omega_0 = 135^\circ$. This leaves us with just two parameters to vary, namely e and K .

Given e and K we generate N_{obs} data-points with times t_i uniformly distributed⁸ within a period and then we add to each time a random number of periods between 0 and 20. For transiting exoplanets the observations would have to be taken uniformly in time intervals excluding the transit. We then get the observed radial velocity from equation 9 as

$$v_r(t_i) = K[\cos(\omega_0 + f(t_i)) + e \cos(\omega_0)] + G(0, \sigma_{\text{tot}}) \quad (11)$$

where $G(0, \sigma_{\text{tot}})$ is a random Gaussian deviate with mean 0 and standard deviation σ_{tot} . The latter quantity is obtained as $\sigma_{\text{tot}}^2 = \sigma_{\text{obs}}^2 + \sigma_{\text{jitter}}^2$, where σ_{obs} is the random uncertainty for each measurement and σ_{jitter} is the noise arising from stellar jitter. Given the form of equation 9 a Fisher matrix analysis implies that the uncertainty in the longitude of periastron, σ_{ω} satisfies the following scaling

$$\sigma_{\omega} \propto N_{\text{obs}}^{-1/2} \sigma_{\text{tot}} K^{-1}. \quad (12)$$

This scaling allows us to perform a set of fiducial simulations for several values of e and use the results to scale to parameters relevant to a given situation of interest. We note that the simulations we performed verify that the scaling inferred from a Fisher matrix analysis is accurate. In order to measure the longitude of periastron ω with a reasonable degree of certainty the system clearly needs to have a significant amount of eccentricity. We restrict ourselves to systems with $e \geq 0.1$ and we simulate systems with $e = 0.1, 0.2, 0.3, 0.4, 0.5, 0.6$.

For σ_{obs} we assume a typical high-precision measurement with $\sigma_{\text{obs}} = 2$ m sec⁻¹. For the stellar jitter, we perform our fiducial simulations for a typical jitter of $\sigma_{\text{jitter}} = 4$ m sec⁻¹ (Wright 2005; Butler et al. 2006). The limitations imposed by active stars and/or different precision on the radial velocity measurements on the recovery of $\dot{\omega}_{\text{GR}}$ can be explored by using the scaling of σ_{ω} with higher assumed values of σ_{jitter} and/or σ_{obs} . Even though Equation 12 renders multiple values of K redundant, we choose to present results for two values of K for illustrative purposes, namely $K = 100$ m sec⁻¹ and $K = 1000$ m sec⁻¹. The former corresponds roughly to Jupiter-mass exoplanets and is fairly representative of currently known systems (Butler et al. 2006)⁹, while the latter corresponds to super-massive planets which as we will see are the class of systems which would allow the detection of $\dot{\omega}_{\text{GR}}$ with radial velocities. Finally, we do our fiducial simulations for $N_{\text{obs}} = 100$, a value not atypical for well-sampled radial velocity curves available today.

The results of the simulations are summarized in Table 2. From left to right, the columns in this Table record the assumed radial velocity amplitude K , the system eccentricity e , the expected uncertainty in the longitude of periastron

⁸ We ignore in our simulations the Rossiter-McLaughlin effect for the case of transiting planets (Rossiter 1924; McLaughlin 1924; Queloz et al. 2000).

⁹ See also <http://www.exoplanet.eu>.

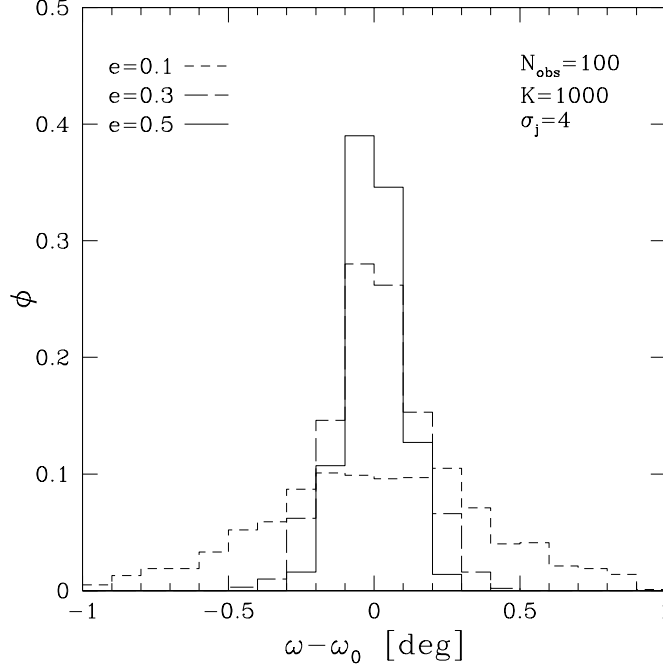


FIG. 1.— Distribution ϕ of recovered angles of periastron $\omega - \omega_0$, where ω_0 is the input angle, for the simulation with $N_{\text{obs}} = 100$, $K = 1000 \text{ m sec}^{-1}$ and $\sigma_j = 4 \text{ m sec}^{-1}$. The distributions are shown for eccentricities $e = 0.1, 0.3, 0.5$.

σ_ω for the simulated system, and finally α_{20} , which we define to be the value of $\dot{\omega}$ that would be necessary in order to achieve a 3σ detection in the simulated systems in a time-span of 20 years when measuring ω in two epochs, each having N_{obs} observations. We note that we have performed Shapiro-Wilk normality tests in the recovered ω distributions. We found that all of them are consistent with normality and thus we are justified in using the dispersion σ_ω to derive confidence levels.

As an example, we show in Figure 1 the distributions of recovered ω for the case with $N_{\text{obs}} = 100$, $K = 1000 \text{ m sec}^{-1}$ and $\sigma_j = 4 \text{ m sec}^{-1}$ for eccentricities $e = 0.1, 0.3, 0.5$. In the upper panel of Figure 2 we show the radial velocity curve for a system with $K = 1000 \text{ m sec}^{-1}$, $e = 0.5$ and $\omega = 135^\circ$, while in the lower panel we show the difference between that curve and a radial velocity curve having $\omega = 136^\circ$. The simulations presented in Table 2 show that this difference can be detected at the $10\text{-}\sigma$ level ($\sigma_\omega \sim 0.1^\circ$) when using $N_{\text{obs}} = 100$ observations, each having an uncertainty of $\sim 2 \text{ m sec}^{-1}$. The high level of significance can be achieved in this case thanks to the assumed low-level of jitter and the super-massive nature of a system with that semi-velocity amplitude.

In order to validate our simulations against uncertainty estimates obtained with real data, we have run a simulation with $N_{\text{obs}} = 20$, $e = 0.517$, $K = 1011 \text{ m sec}^{-1}$, $\omega = 179.3^\circ$ and $\sigma_j = 60 \text{ m sec}^{-1}$. These observational conditions and orbital parameters are appropriate for the observations of HAT-P-2 b reported by Bakos et al. (2007). Our simulations for this case return $\sigma_\omega = 3.8^\circ$, while Bakos et al. (2007) report $\omega_{\text{HAT-P-2b}} = 179.3 \pm 3.6^\circ$, in very good agreement with our estimate. We conclude that our simulations return realistic estimates of the uncertainties in ω .

The simulations presented in Table 2 show that in some cases the precession of periastron detectable in 20 years, α_{20} , is comparable to the values $\dot{\omega}_{GR}$ of currently known systems listed in Table 1. For close-in, eccentric, super-massive planets ($K \sim 1000 \text{ m sec}^{-1}$) about 100 observations per epoch are sufficient, while for Jupiter-mass exoplanets ($K \sim 100 \text{ m sec}^{-1}$) an unrealistically large number of radial velocity observations, $N_{\text{obs}} = 10000$ per epoch, would be needed. Therefore, observations of different epochs of radial velocities with a time-span of ~ 20 years would detect the variations in the precession of exoplanet periastra induced by GR in some currently known super-massive systems. The estimates above assume a typical level of stellar jitter. For active stars the number of observations have to be increased in proportion to the dispersion characterizing the jitter (see Equation 12). Stellar activity is therefore an important limitation to detect changes in ω using radial velocities. All in all, radial velocity studies of exoplanets will be generally able to ignore the effects of GR precession as they will usually be well below a detectable level.

We note in closing that Miralda-Escudé (2002) and Heyl & Gladman (2007) consider using radial velocities and transit timing observations in order to measure the small difference between the period observed in the radial velocities and the period between primary transits. Both works conclude that this is not a competitive method and so we will not consider it further here and refer the reader to those works for details.

3.2. Duration of Transits

As the planetary orbit acquires a significant eccentricity e , the duration of the primary and secondary transits are no longer equal and acquire a dependence on the longitude of periastron of the system. An explicit expression for

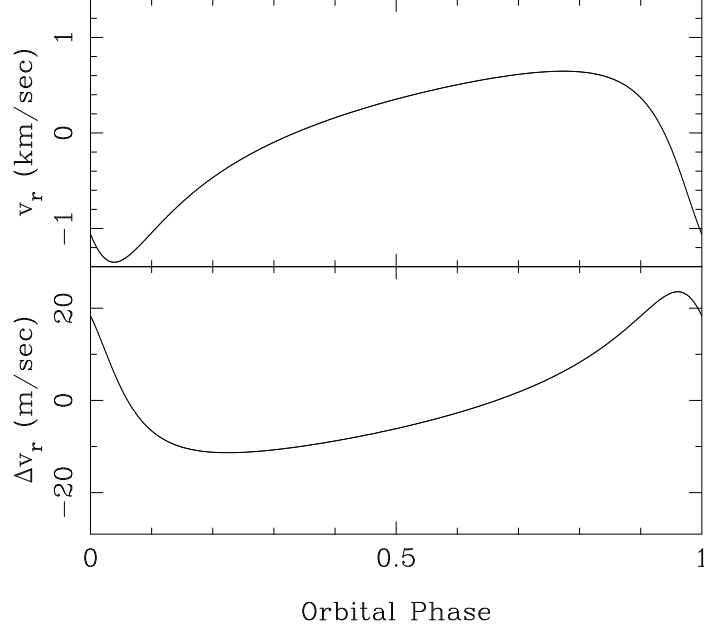


FIG. 2.— (Top) Radial velocity curve as a function of orbital phase for a system with $K = 1000 \text{ m sec}^{-1}$, $e = 0.5$ and $\omega = 135^\circ$. (Bottom) Difference between the curve in the top panel and a radial velocity curve that is identical except in that it has $\omega = 136^\circ$. Note the different y -axis scales used in the different panels.

the duration of a transit D in the eccentric case was derived by Tingley & Sackett (2005, their equation 7) under the assumption that the distance between the planet and the star does not change significantly during transit. It is given by

$$D = 2Z(R_\star + R_p) \frac{\sqrt{1-e^2}}{(1+e\cos(f_t))} \left(\frac{P}{2\pi GM_{\text{tot}}} \right)^{1/3}, \quad (13)$$

where

$$Z = \sqrt{1 - \frac{r_t^2 \cos^2 i}{(R_\star + R_p)^2}} \equiv \sqrt{1 - b^2} \quad (14)$$

is a geometrical factor related to the impact parameter b . R_\star and R_p are the radii of the star and planet respectively, $M_{\text{tot}} \equiv M_\star + M_p$ and r_t and f_t are the radii and true anomaly at the time of transit, respectively. The latter clearly depends linearly on ω and we therefore have $\dot{f}_t = \dot{\omega}$. The logarithmic derivative of the duration of a transit is

$$d \ln D / dt = \frac{\dot{\omega} e \sin(f_t)}{(1+e\cos(f_t))} \left\{ 1 - \frac{b^2}{1-b^2} \right\}. \quad (15)$$

In Figure 3 we show the quantity $(1/\dot{\omega})d \ln D / dt$ for a central transit ($b = 0$) and for $e = 0.1, 0.3, 0.5, 0.7$, with higher e giving higher values of $|(1/\dot{\omega})d \ln D / dt|$. The change in the duration of an eclipse for a small change in ω given by $\dot{\omega} \delta t$ is simply $\delta D \sim D \dot{\omega} \delta t [\dot{\omega}^{-1} d \ln D / dt]$. For $\dot{\omega} \delta t \sim 0.5 \times 10^{-2} \text{ rad}$, appropriate for the expected change in ω for $\dot{\omega}_{\text{GR}} \sim 3 \text{ deg/century}$ over 10 years, we have that $\delta D \sim 0.075 D \times 10^{-2}$ for $e \sim 0.3$, which translates into $\delta D \sim 10 \text{ sec}$ for a transit duration of $D \sim 0.15 \text{ day}$ which is typical for the systems that we explore in this work.

A very interesting feature of Equation 15 is its dependence on the impact parameter b . First, $d \ln D / dt$ vanishes for $b = 1/\sqrt{2}$. This behavior is possible due to two competing effects which cancel out exactly for that value of b : an increase/decrease in the star-planet separation causes both an increase/decrease in the path-length of the planet across the disk of the star and a corresponding decrease/increase in the velocity across it, which implies a slower/faster crossing-time. Secondly, for systems with values of b close to 1 (i.e., near-grazing systems), the value of $d \ln D / dt$ increases greatly. We will come back to near-grazing systems below; in what immediately follows we will quantify the accuracy to which we can determine the transit duration D .

If the times of beginning of ingress and end of egress are denoted by t_i and t_e respectively, then the duration of a transit is given by $D = t_e - t_i$ and the uncertainty in the duration is $\sigma_D^2 = \sigma_{t_i}^2 + \sigma_{t_e}^2$ (assuming no correlation between t_i and t_e). If the ingress has a duration of Δt_i (i.e. the time from first contact to second contact) then a linear approximation of the flux during this time can be written as $F(t) = F_0(1 - (t - t_i)(R_p/R_\star)^2/\Delta t_i)$, where F_0 is the out-of-transit stellar flux and we ignore the effects of limb darkening. If the light curve is being sampled at a rate Γ per unit time then we have $N = \Delta t_i \Gamma$ photometric measurements during the egress. If each photometric measurement has

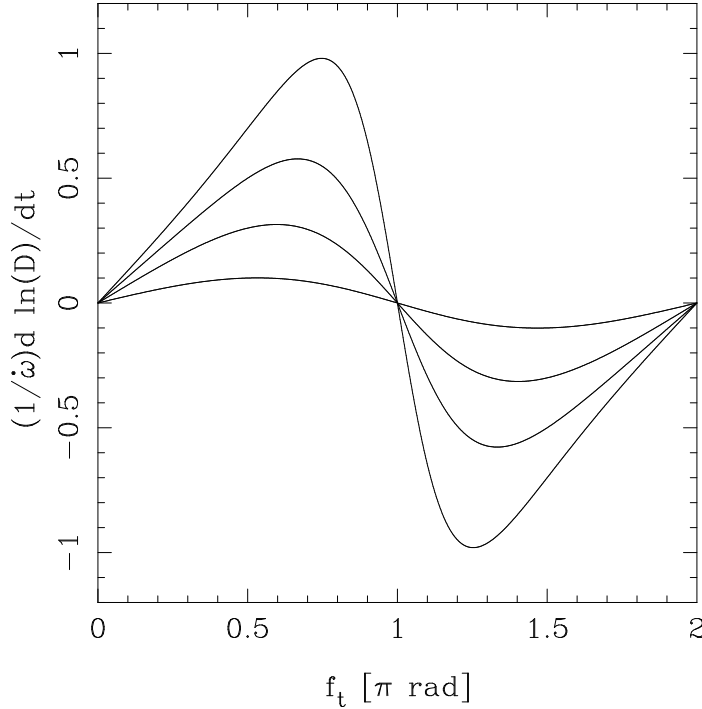


FIG. 3.— $(1/\dot{\omega})d \ln D/dt$ as a function of the true anomaly at the time of transit f_t for a central transit ($p = 0$). The different curves are for difference eccentricities $e = 0.1, 0.3, 0.5, 0.7$, with higher e giving higher values of $|(1/\dot{\omega})d \ln D/dt|$. The extrema in this figure are at values of the true anomaly at the time of transit of $f_t = \pm \arccos(-e)$.

a fractional precision σ_{ph} , and assuming R_p and R_* are known, a least-squares fit to the photometric series will allow the determination of t_i with an uncertainty $\sigma_{t_i} = \sigma_{\text{ph}} \Delta t_i (R_*/R_p)^2 N^{-1/2} = \sigma_{\text{ph}} (\Delta t_i / \Gamma)^{1/2} (R_*/R_p)^2$. The uncertainty in the time of egress is given by a similar expression replacing Δt_i by Δt_e .

If we assume that the ingress and egress times are equal¹⁰, and insert explicit expressions for $\Delta t_i \approx \Delta t_e$ and D , we get that for a central transit (Ford et al. 2008):

$$\frac{\sigma_D}{D} \approx \frac{40.7 \sigma_{\text{ph}} \sqrt{1 + e \cos f_t}}{(1 - e^2)^{1/4}} \sqrt{\frac{2}{N_{tr} \Gamma}} \left(\frac{R_p}{R_{\oplus}} \right)^{-3/2} \left(\frac{R_*}{R_{\odot}} \right) \left(\frac{M_*}{M_{\odot}} \right)^{1/6} \left(\frac{P}{\text{yr}} \right)^{-1/6} (1 + R_p/R_*)^{-3/2}, \quad (16)$$

where N_{tr} is the number of transits observed, Γ is to be expressed in units of min^{-1} , and we have neglected factors including $(1 + \mu)$, where $\mu = M_p/M_*$. We note for later reference that the uncertainty in the central transit time $t_c \equiv 0.5(t_e + t_i)$ is $\sigma_c \approx \sigma_D/\sqrt{2}$.

The highest photometric precision in a transit light curve has been achieved with *HST* (Brown et al. 2001; Pont et al. 2007) with $\sigma_{\text{ph}} \sim 10^{-4}$. For parameters appropriate to HD 209458 Equation 16 gives $\sigma_D \sim 5$ sec. The uncertainties in the central time $\sigma_c \sim \sigma_D$ reported in Brown et al. (2001) are of the same order and we therefore deem Equation 16 to be a reasonable estimate of the expected uncertainties¹¹. We will take this to be the highest precision currently possible for facilities such as *HST* where only a few transits are typically observed.

The *Kepler* mission (Borucki et al. 2003; Basri et al. 2005) will observe $\sim 100,000$ stars continuously with $\sigma_{\text{ph}} \sim 4 \times 10^{-4}$ for a one minute exposure of $V = 12$ solar-like star and expects to find a large number of close-in “hot Jupiters”. The precision attainable in one year for a 1-minute sampling of a Jupiter-mass system with $P = 5$ days orbiting a $V = 12$ solar-type star is $\sigma_D/D \sim 1.1 \times 10^{-4}$ or $\sigma_D \sim 1.5$ sec for a 0.15 days transit duration.

Kepler should therefore be capable of detecting changes in the transit duration D due to GR within its mission for some eccentric, close-in systems, and certainly when coupled to follow-up determinations of D with a facility delivering a precision similar to what *HST* can achieve. Of particular interest will be systems that are near-grazing, due to the factor of $(1 - b^2)^{-1}$ in Equation 15. If eccentric, close-in, near-grazing systems are found in the *Kepler* CCDs, they will be subject to significant changes in D which should be observable. For example, a system with $e = 0.4$, $b = 0.85$, $f_t = \pi/2$ and $\dot{\omega}_{\text{GR}} \sim 3$ deg/century would have a change in D of ~ 9 sec during *Kepler*’s lifetime for $D = 0.075$ days, a change which would be detectable. Of course, as b approaches one, D will tend to zero and the assumptions leading to Equation 16 will break down and make the estimated uncertainty optimistic, both effects which will counter the

¹⁰ The ingress and egress times are not equal in general for eccentric systems, see Equation 7 in Ford et al. (2008). This small difference has no significant effect on the uncertainty estimates dealt with here.

¹¹ We note that Brown et al. (2001) warn about the presence of systematic effects not accounted for in the Poisson uncertainty estimate that could be of the same order as σ_D for their observations.

corresponding increase of $d \ln D / dt$.

3.3. Period Between Transits

As already noted by Miralda-Escudé (2002) and Heyl & Gladman (2007), as the longitude of periastron changes, the period between transits P_t will change as well. Periods are the quantities that are measured with the greatest precision, usually with uncertainties on the order of seconds from ground-based observations (e.g., the average uncertainty for HATNet planets discovered to date is 4.5 seconds).

To first order in e the derivative of the transit period is given by

$$\dot{P}_t = 4\pi e \left(\frac{\dot{\omega}_{\text{GR}}}{n} \right)^2 \sin(M_t) \quad (17)$$

where M_t is the mean anomaly at transit (Miralda-Escudé 2002) and is related to the true anomaly at transit f_t to first order in e by $M_t = f_t - 2e \sin f_t$. For $e = 0.1$, a 5 day period, and $\dot{\omega}_{\text{GR}} = 3$ deg/century, the root mean square value of dP_t/dt over all possible M_t values is $\sim 10^{-12}$, which translates into a period change of $\sim 2 \times 10^{-4}$ sec in 10 years. The period can be determined to a precision $\sim \sigma_c N_{tr}^{-3/2}$ or $\sigma_D N_{tr}^{-1} 2^{-1/2}$ using the expression for σ_D above¹². Assuming the parameters for *Kepler* as above ($V = 12$ star, $P = 5$ day period) the precision achievable during 1 year is ~ 0.013 sec.

Based on the numbers above we conclude that measuring significant changes in the transiting period in $\lesssim 10$ years timescales is not feasible. Our conclusions are in broad agreement with the analysis presented in Miralda-Escudé (2002) and Heyl & Gladman (2007), who conclude that thousands of transits need to be observed with high precision in order to detect significant variations in P_t . As there is no existing or planned facility that will allow to observe this amount of transits with the required photometric precision we conclude that measurements of \dot{P}_t will not be significantly affected by changes in ω of the magnitudes expected to arise from GR or from the secular changes due to a perturber.

3.4. Time Between Primary and Secondary Transit

In the case where the exoplanet is transiting it may be possible to observe not only the primary transit, i.e. the transit where the exoplanet obscures the host star, but also the occultation, when the host star blocks thermal emission and reflected light from the exoplanet (e.g., Charbonneau et al. 2005). If the time of the primary eclipse is given by t_1 and that of the secondary by t_2 , the time difference between the two as compared to half a period P , $\Delta t \equiv t_2 - t_1 - 0.5P$, depends mostly on the eccentricity e and the angle of periastron ω . Indeed, an accurate expression that neglects terms proportional to $\cot^2 i$ where i is the inclination angle and is therefore exact for central transits, is given by

$$\Delta t = \frac{P}{\pi} \left(\frac{e \cos(\omega) \sqrt{1 - e^2}}{(1 - (e \sin \omega)^2)} + \arctan \left(\frac{e \cos \omega}{\sqrt{1 - e^2}} \right) \right) \quad (18)$$

(Sterne 1940). Combined with radial velocities this time difference offers an additional constrain on e and ω , and in principle a measurement of Δt combined with a measurement of the difference in the duration of the secondary and primary eclipses can be used to solve for e and ω directly (see discussion in Charbonneau et al. 2005). We note that Heyl & Gladman (2007, their §4.2) also consider secondary transit timings as a means to measure changes in ω . While their discussion is based on first order expansions in e instead of using the exact expression above and is phrased in different terms, it is based ultimately on the same measurable quantity we discuss here.¹³

Equation 18 does not include light travel time contributions, i.e. it neglects the time it takes for light to travel across the system. This time is given for a central transit by

$$\Delta_{t,LT} = \frac{2a(1 - e^2)}{c[1 - (e \cos f_t)^2]}, \quad (19)$$

where f_t is the true anomaly at the time of primary transit. In this section we will be interested in changes in Δt due to changes in ω . It is easy to see from the expressions above that $d\Delta_{t,LT}/d\omega \ll d\Delta t/d\omega$ (ignoring the points where they are both zero). Therefore, changes in the time difference between primary and secondary transits will be dominated by changes in Δt and we can safely ignore light travel time effects in what follows.

The precession of periastra caused by GR will change ω systematically, while leaving e unchanged. Therefore Δt has the potential of offering a direct measurement of changes in ω . We use Equation 18 to calculate $(1/P)d\Delta t/d\omega$ as a function of ω . The result is shown in in Figure 4 for $e = 0.1, 0.3, 0.5, 0.7$, with higher e yielding larger extrema of $|(1/P)d\Delta t/d\omega|$.

¹² The scaling $N^{-3/2}$ follows from describing the central transit times as $t_i = t_0 + Pi$, with $i = 1, \dots, N_{tr}$ and determining P using a χ^2 fit. The variance in the derived P is (see, e.g., Gould 2003) $\sigma_P^2 \approx (3/N^3)\sigma_c^2 + \mathcal{O}(N^{-4})$.

¹³ Heyl & Gladman (2007) consider the time difference between successive primary transits (Δt_0) and successive secondary (Δt_π) transits, following their notation. This difference can be expressed as $\Delta t_0 - \Delta t_\pi \approx -(d\Delta t/d\omega)\delta\omega$, where Δt is the quantity defined in Equation 18 and $\delta\omega$ is the change in ω in one orbit.

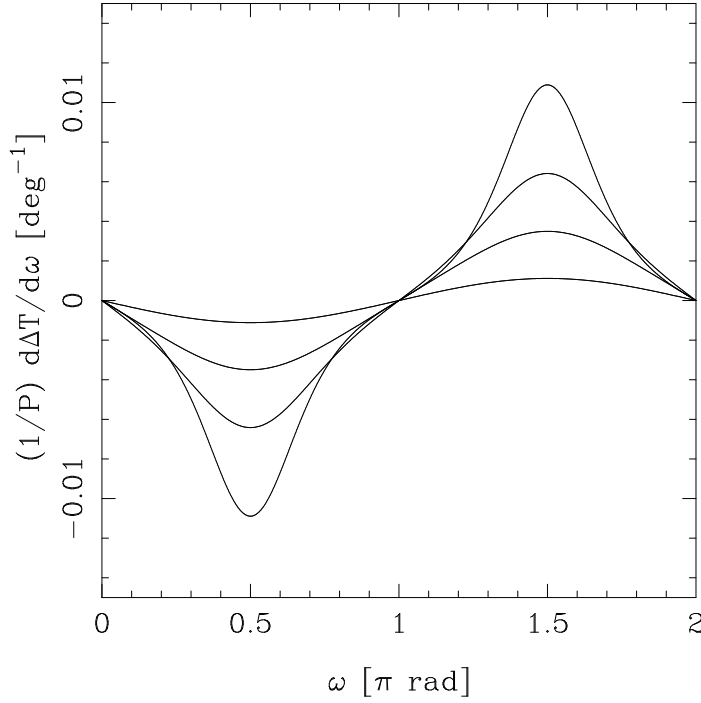


FIG. 4.— $(1/P)d\Delta t/d\omega$ as a function of ω . The different curves are for different eccentricities $e = 0.1, 0.3, 0.5, 0.7$, with higher e giving larger extrema of $|(1/P)d\Delta t/d\omega|$.

If $\omega \approx \pi/2$ or $\approx 3\pi/2$, the changes Δt in a system with $P = 4$ days for 0.2 degrees of precession would be large, on the order of 8 min for $e \sim 0.5$. Published observations of secondary eclipses with *Spitzer* constrain t_2 to within ~ 80 sec (Deming et al. 2006; Harrington et al. 2007; Charbonneau et al. 2008). Uncertainties in t_2 will dominate the uncertainty in Δt , so we assume $\sigma_{\Delta t} \approx \sigma_{t_2} \sim 80 N_{tr}^{-3/2}$ sec, where N_{tr} is the number of secondary transits observed.

Determining Δt at two epochs separated by 10 years and observing $N_{tr} \sim 1$ at each epoch with a facility like *Spitzer* would detect the changes in Δt due to GR with a significance $\gtrsim 4\sigma$ in an eccentric system that precesses $\gtrsim 0.2$ deg in a decade if they have ω around $\pi/2$ or $3\pi/2$. While *Spitzer* is now entering the end of its cryogenic lifetime, future facilities might be able to achieve similar precision. Moreover, as new suitable systems are discovered with very hot atmospheres (pM class planets, Fortney et al. 2007) observations of secondary transits might be feasible from the ground (López-Morales & Seager 2007).

Finally, we note that since $f_t = \pm\pi/2$ when $\omega = 0$ or π , measuring the change in Δt complements measurements of changes in primary transit duration D , in the sense that when one effect is not operating the other one generally is.

4. ASSESSING THE DIFFERENT CONTRIBUTIONS TO $\dot{\omega}$

If a change in ω is detected using any of the methods described above it would be interesting to determine its likely cause. As mentioned in § 2, the contribution to $\dot{\omega}$ from a second planet or tidal deformations can be of comparable magnitude to that caused by GR, making the origin of a potential detection of a change in ω unclear unless the presence of a perturber and the magnitude of tidal effects can be assessed. In this section we address three points. First, we discuss how may one assess if part of a detected change in ω comes from a perturber. Secondly, we show that the a terrestrial mass ($M_{\oplus} \lesssim M \lesssim 10$) perturber may be detectable through the induced secular changes in ω over the value expected from GR and tidal deformations by using transit and radial velocity observations. Finally, we assess the relative contributions of GR and tidal deformations for the case where perturbers do not contribute significantly to $\dot{\omega}$.

4.1. Constraining Potential Contributions to $\dot{\omega}$ from $\dot{\omega}_{\text{perturber}}$.

First, we note that using a precise radial velocity curve with $N_{\text{obs}} \sim 100$ we can probe the presence of companions with $M \gtrsim 15M_{\oplus}$ (Narayan et al. 2005). As shown in § 2, lower mass companions can still contribute significantly to $\dot{\omega}$, so it would be useful to have further information about possible companions in order to better interpret a measured $\dot{\omega}$. The presence of a second exoplanet in the system will not only cause secular changes in ω as discussed in § 2 (equation 7), but it may cause significant transit-time variations even for perturbers with masses comparable to the earth (Agol et al. 2005; Holman & Murray 2005). The transit-time variations will be on the order of seconds to minutes, depending on the orbital parameters and mass of the perturber. Constant monitoring of transiting exoplanets such as will be performed by *Kepler* will allow to identify systems that show significant transit time variations.

We note that the presence of a perturber will not only change ω but it may also affect other orbital elements such as the orbit inclination (Miralda-Escudé 2002). These small changes in inclination have indeed been proposed

as a method of detecting terrestrial mass companions in near-grazing transit systems which are especially sensitive to them (Ribas et al. 2008). Following the formalism presented in §6 of Murray & Dermott (1999) we expect that secular changes to e by a perturber satisfy $|de/dt| \lesssim (3/16)n(a/a_2)^3(M_2/M_\star)e_2$, where a_2, e_2 and M_2 are the orbital semi-major axes, eccentricity and mass of the perturber respectively. For $e_2 = 0.1$, $a_2 = 2a$ and $M_2 = 3 \times 10^{-6}M_\star$ we have that $de/dt \lesssim 4 \times 10^{-6} \text{ yr}^{-1}$ for a system with $P = 4$ days. This is too small for changes in e to be detected with radial velocities in scales of tens of years and so we conclude that secular changes in eccentricities induced by perturbers will in general not be useful to infer the presence of perturbers.

Summarizing, the best way to try to constrain contributions of $\dot{\omega}_{\text{perturber}}$ to a detected change in ω is to consider transiting systems possessing extensive photometric monitoring, allowing to probe the existence of transit time variations. For near-grazing systems, the same photometric monitoring would additionally allow to probe for small changes in i due to a perturber.

4.2. Using Secular Variations in ω to Detect Terrestrial Mass Planets.

A very interesting possibility raised by the secular variation in ω induced by a “perturber” is to use these variations in order to infer the presence of terrestrial mass planets. This possibility was studied by Miralda-Escudé (2002) and then followed-up by Heyl & Gladman (2007). Secular variations in ω , especially through their effect on transit durations (§ 3.2), can offer an interesting complement to transit time variations as a means of detecting terrestrial mass planets in the upcoming *Kepler* mission.

As we have seen in § 2, the precession due to GR and tidal deformations can be of comparable magnitude to that induced by a terrestrial mass perturber. It is germane to ask then to what extent will the uncertainty in the expected value of $\dot{\omega}_{\text{GR}}$ and $\dot{\omega}_{\text{tide}}$ limit the detectability of a perturber.

We start by considering $\dot{\omega}_{\text{GR}}$. The fractional uncertainty in $\dot{\omega}_{\text{GR}}$ is given by $(\sigma(\dot{\omega}_{\text{GR}})/\dot{\omega}_{\text{GR}})^2 = (\sigma(M_\star)/M_\star)^2 + (\sigma(a)/a)^2 + (\sigma(P)/P)^2 + 4e^2(\sigma(e)/(1-e^2))^2$, where we have ignored correlations. The fractional uncertainty in P is generally negligible, while the other quantities can be typically of the order of a few percent. We will therefore assume that $\sigma(\dot{\omega}_{\text{GR}})/\dot{\omega}_{\text{GR}} \sim 10\%$. It follows that to detect an excess precession caused by a perturber we need at least that $\dot{\omega}_{\text{perturber}} - \dot{\omega}_{\text{GR}} \gtrsim 0.3\dot{\omega}_{\text{GR}}$. It is easy to see that if $\dot{\omega}_{\text{perturber}} \gtrsim \dot{\omega}_{\text{GR}}$ and $\dot{\omega}_{\text{perturber}}$ is itself detectable, i.e. $\dot{\omega}_{\text{perturber}} > 3\sigma_{\dot{\omega}}$, where $\sigma_{\dot{\omega}}$ is the uncertainty in the measured $\dot{\omega}$, then the uncertainty in the expected $\dot{\omega}_{\text{GR}}$ will not spoil the significance of the detection. Using the equations presented in § 2 we get that

$$\frac{\dot{\omega}_{\text{perturber}}}{\dot{\omega}_{\text{GR}}} = \frac{3.8}{(1-e^2)} \left(\frac{M_\odot}{M_\star}\right)^2 \left(\frac{a}{a_2}\right)^3 \left(\frac{a}{0.05\text{AU}}\right) \left(\frac{M_2}{M_\oplus}\right). \quad (20)$$

It is clear from this expression that for typical values of $M_\star \sim M_\odot$, $a \sim 0.05 \text{ AU}$, $e \lesssim 0.5$ there will be values of a_2 for which we have $\dot{\omega}_{\text{perturber}} > \dot{\omega}_{\text{GR}}$ and for which the uncertainty in the expected precession from GR will not be a limiting factor in detecting terrestrial mass perturbers.

We consider now $\dot{\omega}_{\text{tide}}$. The fractional uncertainty considering all parameters excepting $k_{2,p}$ and \mathcal{T} and ignoring correlations is $(\sigma(\dot{\omega}_{\text{tide}})/\dot{\omega}_{\text{tide}})^2 = (\sigma(P)/P)^2 + (5\sigma(R_p/a)/(R_p/a))^2 + (\sigma(M_p/M_\star)/(M_p/M_\star))^2 + (f'(e)\sigma(e)/f(e))^2$. We have expressed this in terms of the ratios M_p/M_\star and R_p/a as these quantities are more robustly determined observationally. As was the case above, the uncertainties in the variables can be typically a few percent and we therefore assume that $\sigma(\dot{\omega}_{\text{tide}})/\dot{\omega}_{\text{tide}} \sim 10\%$. Using the equations presented in § 2 we get that

$$\frac{\dot{\omega}_{\text{perturber}}}{\dot{\omega}_{\text{tide}}} = \frac{1.85}{\mathcal{T}f(e)k_{2,p}} \left(\frac{M_\odot}{M_\star}\right)^2 \left(\frac{a}{a_2}\right)^3 \left(\frac{a}{0.05\text{AU}}\right)^5 \left(\frac{R_J}{R_p}\right)^5 \left(\frac{M_p}{M_J}\right) \left(\frac{M_2}{M_\oplus}\right). \quad (21)$$

In the case of $\dot{\omega}_{\text{tide}}$ we cannot measure the apsidal motion constant k_2 . As discussed in § 2, the value of k_2 for a giant planet is expected to be close to the extreme value of a uniform sphere, so we can conservatively assume $k_{2,p} = 0.75$, a value that maximizes the expected $\dot{\omega}_{\text{tide}}$. For a close-in Jupiter we have $\mathcal{T} \approx 1$. Using these values and following the same reasoning as for $\dot{\omega}_{\text{GR}}$, it is clear from the expression above that for typical values of $M_\star \sim M_\odot$, $a \sim 0.05 \text{ AU}$, $e \lesssim 0.5$, $R_p \sim R_J$, $M_p \sim M_J$, there will be values of a_2 for which we have $\dot{\omega}_{\text{perturber}} > \dot{\omega}_{\text{tide}}$ and for which the uncertainty in the expected precession arising from tidal deformations will not be a limiting factor in detecting terrestrial mass perturbers. Note that due to the strong dependence on a , tides may become a limiting factor for very close-in systems.

We consider now the detectability of $\dot{\omega}_{\text{perturber}}$ with *Kepler* using the change in the transit duration D . As discussed in § 3.2, a 1-minute sampling of a Jupiter-mass system with *Kepler* for a $P = 5$ days planet orbiting a $V = 12$ solar-type star will achieve a precision of $\sigma_D \sim 1.5 \text{ sec}$ for a 0.15 days transit duration. We therefore set a change of 6 sec over 4 years to constitute a detectable δD for this system, which translates into a detectable $\dot{\omega}$ of $\dot{\omega}_{\text{detect}} = 6/(D\Delta t(\dot{\omega}^{-1}d\ln D/dt))$, where $\Delta t = 4$ years and we assume a central transit (see Equation 15).

We show in Figure 5 the expected value of $\dot{\omega}_{\text{perturber}}$ as a function of a_2/a assuming $a = 0.05 \text{ AU}$, $M_\star = M_\odot$, and $f_t = 0.5\pi$ as solid lines, one for $M_2 = M_\oplus$ and another for $M_2 = 10M_\oplus$. The dashed line marks the values of $\dot{\omega}_{\text{detect}}$ for $e = 0.4$. The dotted lines mark the values of $0.3\dot{\omega}_{\text{GR}}$ for the same eccentricity, while the dash-dot-dot line marks $0.3\dot{\omega}_{\text{tide}}$. This figure shows that over a range of values of (a_2/a) *Kepler* may be able to detect the presence of additional super-Earths ($M_\oplus \lesssim M \lesssim 10M_\oplus$) if the primary planet has a favorable impact parameter and true anomaly at the time of transit.

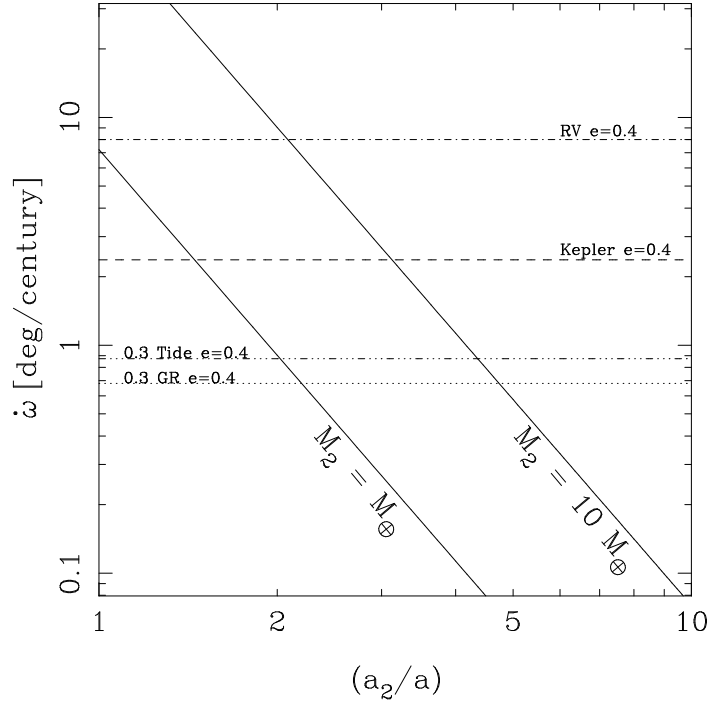


FIG. 5.— The solid lines show the expected value of $\dot{\omega}_{\text{perturber}}$ as a function of a_2/a for $M_2 = M_\oplus$ and $M_2 = 10M_\oplus$, assuming $a = 0.05$ AU, $M_\star = M_\odot$ and $f_t = 0.5\pi$. The dashed line marks the lower value of $\dot{\omega}$ that is detectable with *Kepler* for $e = 0.4$ via the changes in transit duration. The dotted line marks the value of $0.3\dot{\omega}_{\text{GR}}$ for the same eccentricity, while the dash-dot-dot line marks $0.3\dot{\omega}_{\text{tide}}$. Finally, the dot-dashed line marks the lower values of $\dot{\omega}$ that would be detectable with 100 radial velocities at each of two epochs separated by 5 years, for a perturber to a super-massive $M_1 = 10M_J$ primary planet orbiting an inactive solar-mass star (see text for more details).

Finally, we consider the detectability of $\dot{\omega}_{\text{perturber}}$ using radial velocities alone. We assume the primary planet is a super-massive system of $M_p = 10M_J$, with the rest of the star and orbital parameters as assumed above. The results of § 3.1 show that with 100 radial velocity observations at each epoch a precession of ~ 8 deg/century could be detected (at 3σ) in 5 years if the system has $e = 0.4$ and orbits an inactive star. We mark the detectable level in this case with radial velocities as dot-dashed line in Figure 5. From this Figure we can see that if enough observations are in hand, perturbing planets with masses $\sim 10M_\oplus$ may be detectable with radial velocities alone for the case of super-massive systems orbiting inactive stars.

We conclude that measuring the precession of ω caused by a perturber above the value predicted by GR and tidal effects may lead to detection of additional planets with both transit and radial velocity observations (for transits, see also Miralda-Escudé (2002); Heyl & Gladman (2007)). The examples given above are illustrative only; a detailed analysis is beyond the scope of this work. Of special interest will be to estimate the yield of terrestrial-mass planets expected from *Kepler* by measuring secular changes in transit durations.

4.3. The Relative Magnitude of $\dot{\omega}_{\text{GR}}$ and $\dot{\omega}_{\text{tide}}$.

If there are no perturbers causing significant changes in ω , these changes will be caused by a combination of GR and tidal deformations. We now briefly consider the relative magnitudes of these effects. Using the equations presented in § 2 we find that

$$\frac{\dot{\omega}_{\text{GR}}}{\dot{\omega}_{\text{tide}}} = \frac{4.8}{\mathcal{T}(1-e^2)f(e)} \left(\frac{0.1}{k_{2,p}} \right) \left(\frac{a}{0.05\text{AU}} \right)^4 \left(\frac{R_J}{R_p} \right)^5 \left(\frac{M_p}{M_J} \right). \quad (22)$$

For expected values of $k_{2,p} \sim 0.25$ and assuming $R_p \sim R_J$, $M_p \sim M_J$, $a \sim 0.05$ and $e \lesssim 0.5$ we see that the values of $\dot{\omega}_{\text{GR}}$ and $\dot{\omega}_{\text{tide}}$ are comparable. Note that there is a very strong dependence on a . For smaller values of a , a regime where the precession due to GR would offer better chances of being observable for eccentric systems, the contribution from tidal deformations may quickly become the dominant source of precession. The fact that the tidal contributions to the precession are expected to be generally significant limits the ability to directly extract the precession due to GR. The magnitude of the precession caused by tidal deformations is uncertain due to the need to know the planetary structure. Given that the expected precession due to GR is unambiguous, in systems where the precession due to tidal deformations is expected to be dominant *and* detectable, we might be able to learn about the tidally driven precession of ω by subtracting the effects of GR from a measured $\dot{\omega}$.

5. ANALYSIS OF SPECIFIC SUPER-MASSIVE SYSTEMS

As illustration of the material discussed above, we analyze now in some detail two currently known systems that due to their large measured velocity amplitudes have the potential to have a measurable $\dot{\omega}$ using all the techniques

presented above: HAT-P-2 b (Bakos et al. 2007; Loeillet et al. 2008) and XO-3 b (Johns-Krull et al. 2008).

5.1. HAT-P-2 b

HAT-P-2 b is an especially interesting system due to its very high eccentricity, high mass of $\approx 9M_J$ and close orbit ($a = 0.0677$ AU) to its host star. As shown in Table 1 its value of $\dot{\omega}_{\text{GR}}$ is $\sim 2^\circ/\text{century}$, while the expected value of $\dot{\omega}_{\text{tide}}$ is ~ 0.25 deg/century assuming $k_{2,p} = 0.25$. Unfortunately it has a high level of stellar jitter, with estimates ranging from 17 m sec^{-1} to 60 m sec^{-1} (Bakos et al. 2007; Loeillet et al. 2008). So even though this system has $K \sim 1000 \text{ m sec}^{-1}$ it would require an unrealistically large number of observations ($\sim 10^4$) per epoch in order to make its expected $\dot{\omega}_{\text{GR}}$ detectable with radial velocities.

The value of ω derived for HAT-P-2 b is 1.05π and we therefore would not expect to see significant variations in the time between primary and secondary transits in case the secondary transit was observed (see Figure 4). With $\omega = 1.05\pi$ the true anomaly at the time of transit will be $f_t \approx 0.45\pi$, or 1.55π . Given that the impact parameter is $b \approx 0$ we get from Equation 15 that $|d \ln D / dt| \sim 1.67 \times 10^{-2} \text{ century}^{-1}$. Using the fact that $D = 0.15$ days we expect then a change of ~ 21 sec in D over 10 years due to GR. This difference could be readily detected with high precision photometric observations that determine D to within a few seconds such as is possible with *HST*. The observations currently available constrain D only to within ~ 3 mins (Bakos et al. 2007), and so no first epoch suitable to measuring changes in D is yet in hand.

5.2. XO-3 b

As shown in Table 1 XO-3 b has the largest predicted $\dot{\omega}_{\text{GR}}$ of all currently known exoplanets with $e > 0.1$. While its eccentricity is not as high as that of HAT-P-2 b, it is more massive and orbits closer to its host star XO-3 (also known as GSC 03727-01064). Assuming $k_{2,p} = 0.25$, the expected value of $\dot{\omega}_{\text{tide}}$ is ~ 11 deg/century, about three times as much as the contribution from GR.

In order to assess the detectability of $\dot{\omega}$ with radial velocities for XO-3 b we need to know σ_{jitter} , but unfortunately the precision of the radial velocity measurements presented in Johns-Krull et al. (2008) is too coarse to allow a determination of this quantity ($\sigma_{\text{obs}} \gtrsim 100 \text{ m sec}^{-1}$). Based on the spectral type F5V and $v \sin i = 18.5 \pm 0.2 \text{ km sec}^{-1}$ of XO-3 b (Johns-Krull et al. 2008) we can expect it to have a rather high value of stellar jitter $\sigma_{\text{jitter}} \gtrsim 30 \text{ m sec}^{-1}$ (Saar et al. 1998). Therefore, and just as is the case for HAT-P-2 b, we do not expect $\dot{\omega}$ to be detectable with radial velocity observations due to the expected jitter.

The value of ω derived for XO-3 b is consistent with 0 and we therefore would not expect to see variations in the time between primary and secondary transits in case the secondary transit was observed (see Figure 4). As $\omega \approx 0$, the true anomaly at the time of transit will be $f_t \approx \pi/2$ or $3\pi/2$. Given that the impact parameter is $b \approx 0.8$ we get from Equation 15 that $|d \ln D / dt| \sim 3.56 \times 10^{-2} \text{ century}^{-1}$. Using the fact that $D = 0.14$ days we expect then a change of ~ 43 sec in D over 10 years. Just as is the case for HAT-P-2 b, this could be detectable with determinations of D to within a few seconds and there is no suitable first epoch yet in hand.

6. CONCLUSIONS

In this work we have studied the observability of the precession of periastra caused by general relativity in exoplanets. We additionally consider the precession caused by tidal deformations and planetary perturbers, which can produce a precession of comparable or greater magnitude. We consider radial velocities and transit light curve observations and conclude that for some methods precessions of the magnitude expected from GR will be detectable in timescales of ~ 10 years or less for some close-in, eccentric systems. In more detail, we find that:

1. For transiting systems, precession of periastra of the magnitude expected from GR will manifest itself through detectable changes in the duration of primary transit (§3.2) or through the change in the time between primary and secondary transits (§3.4) in timescales of $\lesssim 10$ years. The two methods are most effective at different values of the true anomaly. A determination of the primary transit duration time to \sim a few seconds and that of the secondary to \sim a minute will lead to measurable effects. The effects of GR and tidal deformations might need to be included in the analysis of *Kepler* data for eccentric, close-in systems. The transit duration of near-grazing systems will be particularly sensitive to changes in ω .
2. Radial velocity observations alone would be able to detect changes in the longitude of periastron of the magnitude expected from GR effects only for eccentric super-massive ($K \sim 1000 \text{ m sec}^{-1}$) exoplanets orbiting close to a host star with a low-level of stellar jitter (§3.1). For the detection to be statistically significant, on the order of 100 precise radial velocity observations are needed at each of two epochs separated by ~ 20 years.
3. Measurements of the change over time of the period between primary transits is not currently a method that will lead to a detection of changes in ω of the magnitude expected from GR (§3.3). Previous works have shown that measuring the small difference between the radial velocity period and that of transits are not sensitive enough to lead to detectable changes due to GR.

In order to contrast any detected change in the transit duration (§3.2) or the time between primary and secondary (§3.4) to the predictions of a given mechanism one needs to know the eccentricity and longitude of periastron of the

systems, for which radial velocities are needed (although not necessarily of the precision required to directly detect changes in ω with them¹⁴). Conversely, photometric monitoring of primary transits are useful in order to elucidate the nature of a detected change in ω by probing for the presence of transit time variations. The presence of the latter would imply that at least part of any observed changes in ω could have been produced by additional planetary companions (§4).

Precession of periastra caused by planetary perturbers and the effects of tidal deformations can be of comparable magnitude to that caused by GR (§2.2). The effects of tidal deformations on the precession of periastra in particular may be of the same magnitude or dominate the total $\dot{\omega}$ in the regime where the GR effects are detectable (§4.3). While this limits the ability to directly extract the precession due to GR given the uncertainty in the expected precession from tides, it might allow to study the tidally induced precession by considering the residual precession after subtracting the effects of GR. The latter possibility is particularly attractive in systems where the tidally induced precession may dominate the signal. We note that even without considering the confusing effects of tidal contributions to the precession, a measurement of $\dot{\omega}_{\text{GR}}$ as described in this work would not be competitive in terms of precision with binary pulsar studies (see, e.g., Will 2006, for a review) and would therefore not offer new tests of GR.

The upcoming *Kepler* mission expects to find a large number of massive planets transiting close to their host stars (Borucki et al. 2003), some of which will certainly have significant eccentricities. Furthermore, systems observed by *Kepler* will be extensively monitored for variations in their transiting time periods in order to search for terrestrial-mass planets using transit-time variations. We have shown that modeling of the transit time durations and further characterization of close-in, eccentric systems might need to take into account the effects of GR and tidal deformations as they will become detectable on timescales comparable to the 4-year lifetime of the mission, and certainly on follow-up studies after the mission ends. We have also shown that planetary companions with super-Earth masses may be detectable by *Kepler* by the change in transit durations they induce (§ 4.2). Additionally, well sampled radial velocity curves spanning $\gtrsim 5$ years may also be able to detect companions with super-earth masses by measuring a change in ω over the expected GR value for the case of super-massive, close-in systems orbiting inactive stars (§ 4.2).

We would like to thank the anonymous referee for helpful suggestions and Dan Fabrycky and András Pál for useful discussions. G.B. acknowledges support provided by the National Science Foundation through grant AST-0702843.

REFERENCES

- Adams, F. C., & Laughlin, G. 2006a, *ApJ*, 649, 992
—, 2006b, *ApJ*, 649, 1004
Agol, E., Steffen, J., Sari, R., & Clarkson, W. 2005, *MNRAS*, 359, 567
Bakos, G. Á., Kovács, G., Torres, G., Fischer, D. A., Latham, D. W., Noyes, R. W., Sasselov, D. D., Mazeh, T., Shporer, A., Butler, R. P., Stefanik, R. P., Fernández, J. M., Sozzetti, A., Pál, A., Johnson, J., Marcy, G. W., Winn, J. N., Sipőcz, B., Lázár, J., Papp, I., & Sári, P. 2007, *ApJ*, 670, 826
Basri, G., Borucki, W. J., & Koch, D. 2005, *New Astronomy Review*, 49, 478
Borucki, W. J., Koch, D. G., Basri, G. B., Caldwell, D. A., Caldwell, J. F., Cochran, W. D., DeVore, E., Dunham, E. W., Geary, J. C., Gilliland, R. L., Gould, A., Jenkins, J. M., Kondo, Y., Latham, D. W., & Lissauer, J. J. 2003, in *Astronomical Society of the Pacific Conference Series*, Vol. 294, *Scientific Frontiers in Research on Extrasolar Planets*, ed. D. Deming & S. Seager, 427–440
Brown, T. M., Charbonneau, D., Gilliland, R. L., Noyes, R. W., & Burrows, A. 2001, *ApJ*, 552, 699
Butler, R. P., Marcy, G. W., Williams, E., Hauser, H., & Shirts, P. 1997, *ApJ*, 474, L115
Butler, R. P., Wright, J. T., Marcy, G. W., Fischer, D. A., Vogt, S. S., Tinney, C. G., Jones, H. R. A., Carter, B. D., Johnson, J. A., McCarthy, C., & Penny, A. J. 2006, *ApJ*, 646, 505
Charbonneau, D., Allen, L. E., Megeath, S. T., Torres, G., Alonso, R., Brown, T. M., Gilliland, R. L., Latham, D. W., Mandushev, G., O'Donovan, F. T., & Sozzetti, A. 2005, *ApJ*, 626, 523
Charbonneau, D., Knutson, H. A., Barman, T., Allen, L. E., Mayor, M., Megeath, S. T., Queloz, D., & Udry, S. 2008, *ArXiv e-prints arXiv:0802.0845*
Claret, A., & Gimenez, A. 1992, *A&AS*, 96, 255
Deming, D., Harrington, J., Seager, S., & Richardson, L. J. 2006, *ApJ*, 644, 560
Ford, E. B., Quinn, S. N., & Veras, D. 2008, *ApJ*, 678, 1407
Fortney, J. J., Lodders, K., Marley, M. S., & Freedman, R. S. 2007, *ArXiv e-prints arXiv:0710.2558*
Goldreich, P., & Soter, S. 1966, *Icarus*, 5, 375
Gould, A. 2003, *ArXiv Astrophysics e-prints astro-ph/0310577*
Harrington, J., Luszcz, S., Seager, S., Deming, D., & Richardson, L. J. 2007, *Nature*, 447, 691
Heyl, J. S., & Gladman, B. J. 2007, *MNRAS*, 377, 1511
Holman, M. J., & Murray, N. W. 2005, *Science*, 307, 1288
Hubbard, W. B. 1984, *Planetary interiors* (New York, Van Nostrand Reinhold Co., 1984, 343 p.)
Johns-Krull, C. M., McCullough, P. R., Burke, C. J., Valenti, J. A., Janes, K. A., Heasley, J. N., Prato, L., Bissinger, R., Fleenor, M., Foote, C. N., Garcia-Melendo, E., Gary, B. L., Howell, P. J., Mallia, F., Masi, G., & Vanmunster, T. 2008, *ApJ*, 677, 657
Loeillet, B., Shporer, A., Bouchy, F., Pont, F., Mazeh, T., Beuzit, J. L., Boisse, I., Bonfils, X., da Silva, R., Delfosse, X., Desort, M., Ecuivillon, A., Forveille, T., Galland, F., Gallenne, A., Hébrard, G., Lagrange, A.-M., Lovis, C., Mayor, M., Moutou, C., Pepe, F., Perrier, C., Queloz, D., Ségransan, D., Sivan, J. P., Santos, N. C., Tsodikovich, Y., Udry, S., & Vidal-Madjar, A. 2008, *A&A*, 481, 529
López-Morales, M., & Seager, S. 2007, *ApJ*, 667, L191
Marcy, G. W., & Butler, R. P. 1996, *ApJ*, 464, L147+
Mayor, M., & Queloz, D. 1995, *Nature*, 378, 355
McLaughlin, D. B. 1924, *ApJ*, 60, 22
Miralda-Escudé, J. 2002, *ApJ*, 564, 1019
Misner, C. W., Thorne, K. S., & Wheeler, J. A. 1973, *Gravitation* (San Francisco: W.H. Freeman and Co., 1973)
Murray, C. D., & Dermott, S. F. 1999, *Solar system dynamics* (Cambridge: Cambridge University Press, 1999)
Narayan, R., Cumming, A., & Lin, D. N. C. 2005, *ApJ*, 620, 1002
Pál, A., & Kocsis, B. 2008, *MNRAS*, in press
Piriaux, S., & Rozelot, J.-P. 2003, *Ap&SS*, 284, 1159
Pont, F., Gilliland, R. L., Moutou, C., Charbonneau, D., Bouchy, F., Brown, T. M., Mayor, M., Queloz, D., Santos, N., & Udry, S. 2007, *A&A*, 476, 1347
Quataert, E. J., Kumar, P., & Ao, C. O. 1996, *ApJ*, 463, 284
Queloz, D., Eggenberger, A., Mayor, M., Perrier, C., Beuzit, J. L., Naef, D., Sivan, J. P., & Udry, S. 2000, *A&A*, 359, L13
Rasio, F. A., Tout, C. A., Lubow, S. H., & Livio, M. 1996, *ApJ*, 470, 1187
Ribas, I., Font-Ribera, A., & Beaulieu, J.-P. 2008, *ApJ*, 677, L59
Rossiter, R. A. 1924, *ApJ*, 60, 15
Saar, S. H., Butler, R. P., & Marcy, G. W. 1998, *ApJ*, 498, L153+
Smeyers, P., & Willems, B. 2001, *A&A*, 373, 173
Sterne, T. E. 1939, *MNRAS*, 99, 451
—, 1940, *Proceedings of the National Academy of Science*, 26, 36
Tingley, B., & Sackett, P. D. 2005, *ApJ*, 627, 1011
Will, C. M. 2006, *Living Reviews in Relativity*, 9
Wright, J. T. 2005, *PASP*, 117, 657
Wu, Y., & Goldreich, P. 2002, *ApJ*, 564, 1024

¹⁴ The eccentricity can be constrained using transit information alone, see Ford et al. (2008)